Supplementary Materials

This PDF file includes:

Supplementary Materials and Methods

Figs. S1 to S7

Tables S1 and S4

Other Supplementary Materials for this manuscript include the following:

Table S2 and S3

MATERIALS AND METHODS

CLINICAL CHARACTERISTICS OF PROBANDS

The CHH cohort included 341 probands (184 KS and 173 normosmic CHH [nCHH]). The diagnosis of CHH was made on the basis of: i) absent or incomplete puberty by 17 years of age; ii) low/normal gonadotropin levels in a setting of low serum testosterone/estradiol levels; and iii) otherwise normal anterior pituitary function and normal imaging of the hypothalamic-pituitary region(*1*). Olfaction was assessed by self-reporting and/or formal testing(*81*). Other CHH-associated phenotypes were evaluated on medical history and physical examination and formally assessed by targeted screening (e.g. audiogram) when possible. When available, family members were included for genetic studies. This study was approved by the ethics committee of the University of Lausanne. All participants provided written informed consent prior to study participation.

Family A, Patient II-1

***NOS1* p.Ala231Thr (heterozygous)**

This male Middle-Eastern proband was first brought to medical attention at age 14-15 years with absent pubertal development, but was ineligible for state-funded healthcare in his country of birth. He had not presented with cryptorchidism or micropenis at birth. He later moved to the United Kingdom and was re-presented to medical services at age 29 years. He remained apubertal (testicular volume at 1-2 ml bilaterally). Congenital hypogonadotropic hypogonadism (CHH) was diagnosed in a setting of low serum testosterone (0.5 nmol/l) and low gonadotropins (LH >0.5 U/l, FSH <0.5 U/l) with otherwise unremarkable pituitary function. Pituitary MRI was normal. The sense of smell was conserved when exposed to basic odorants. Targeted history did not reveal additional phenotypes. His parents were non-consanguineous and their history was unremarkable for pubertal development and sense of smell. The patient does not carry any pathogenic or likely pathogenic variants in known CHH genes. However, he harbors a heterozygous

NOS1 mutation. The origin of this mutation could not be explored, because both parents were unavailable for DNA collection (stateless Bedouinsliving in Kuwait).

Family B, Patient II-1

***NOS1* p.Arg260Gln (heterozygous)**

This male white European anosmic proband was first evaluated for absent puberty at age 15.5 years. Testicular volume was estimated at 1.5 ml bilaterally. Physical examination was unremarkable except for the presence of a supernumerary tooth. Testosterone was frankly low (0.2 nmol/l), accompanied by low gonadotropins (LH 0.1 U/l, FSH 0.6 U/l). A cranial MRI was performed and confirmed pituitary hypoplasia and absent olfactory bulbs. Based on the above data, Kallmann syndrome was diagnosed and testosterone was subsequently started. The patient's mother had normal menarche at age 12 years and was subjectively found to be normosmic on formal testing (UPSIT). The patient's father possibly had delayed puberty but this information could not be verified due to advanced Alzheimer disease and subsequent death. The patient harbors a heterozygous NOS1 mutation, inherited from his mother.

Family C, Patient II-1

***NOS1* p.Thr1107Met (heterozygous)**

This male patient of mixed ethnic origin (Swiss and Libyan) presented with micropenis and right cryptorchidism at birth. An orchidopexy was performed at 9 months of life, coupled with a testicular biopsy that was not suggestive of testicular dysgenesis. At age 12 years, the patient had normal height accrual but did not show any signs of spontaneous puberty. In addition, he reported a decreased sense of smell. Laboratory assessment at that moment showed undetectable serum testosterone associated with low LH and FSH (0.2 and 1.5 U/l), which remained flat following a GnRH stimulation test. A pituitary MRI confirmed the presence of a normal pituitary gland but revealed absent olfactory bulbs bilaterally. The left testicle was not palpable in the scrotum. A pelvic MRI visualized a 0.5

cm testis located in the left inguinal canal, which was subsequently treated by orchidopexy. The patient was started on testosterone replacement at age 13. At age 15, he was reassessed after withdrawal of testosterone replacement. Both testes remained hypotrophic (testicular volume of 0.5 ml with Prader orchidometer). Serum total testosterone was frankly low (0.7 nmol/l) in the presence of undetectable serum LH and FSH without any disturbance in the remaining pituitary axes. A 2-week trial of pulsatile GnRH treatment led to a satisfactory increase of serum gonadotropins (peak of LH and FSH at 7.1 and 6.3 U/l), thus confirming a hypothalamic deficit. Testosterone replacement via intramuscular injection was then reinstated. Normal hearing function was attested by formal testing (audiogram). Family history was remarkable for delayed puberty in the mother whose menarche was induced at age 15.5 years. She later recovered spontaneous menses and was considered to have constitutional delay of growth and puberty (CDGP). The father had a normal pubertal onset. Both parents were found to have a normal sense of smell on formal testing (UPSIT). The patient does not harbor any pathogenic or likely pathogenic variants in known CHH genes. A heterozygous NOS1 mutation was found in both the proband (CHH) and his mother (CDGP).

Family D, Patient II-1

***NOS1*, p.Glu1124Lys (heterozygous)**

This female Middle-Eastern patient presented with complete absence of puberty, manifesting as primary amenorrhea and absent breast development at age 17 years. The diagnosis remained unclear at that moment and the patient was put on estrogen-progestin pills. She was later treated for infertility by ovarian stimulation (gonadotropins) in her country of residence (Kosovo), leading to a triplet pregnancy, but suffered a miscarriage. At age 31 years, she consulted our clinic for a second opinion. After review of previous medical records and a new laboratory assessment confirming isolated hypogonadotropic hypogonadism (estradiol 0.07 nmol/l, LH 0.1 U/l, FSH 0.5 U/l), CHH was suspected. The sense of smell was subjectively conserved but formal testing revealed hyposmia (Sniffin'

Sticks, 10/16, corresponding to 5th percentile). The patient also reported scoliosis. Normal hearing function was attested by formal testing (audiogram). Cranial MRI showed reduced size of the pituitary gland without midline defects. Kallmann syndrome was diagnosed and the patient was subsequently put on pulsatile GnRH replacement, which restored ovulatory cycles and led to a twin pregnancy after 4 cycles. After thorough questioning, her father was found to have delayed puberty (late growth spurt, end of growth at age 19 years). Her mother is anosmic (UPSIT 14/40). The patient's four siblings (two brothers and two sisters) had normal pubertal timing. She gave birth to healthy dizygotic twins (one boy and one girl) with normal genitalia at physical examination. The patient does not carry any variants in known CHH genes but harbors a *NOS1* mutation, inherited from her father (CDGP).

Family E, Patient II-1

***NOS1*, p.Glu1124Lys (heterozygous)**

This male proband of Albanian descent was referred to our center for genetic testing by another Swiss University Hospital. He was diagnosed with CHH at age 19 after consulting for complete absence of pubertal development (absence of male secondary sex characteristics, estimated testicular volume at 1.5 ml, micropenis). At diagnosis, hormonal work-up showed low serum free testosterone at 3 pmol/l (reference range 20.2-99.4 pmol/l), accompanied by undetectable serum LH and FSH (both < 1 U/l). Other causes of hypogonadotropic hypogonadism including hyperprolactinemia were excluded. Pituitary MRI was normal. He was found to have a normal sense of smell on formal testing (UPSIT, 34/40). The patient did not exhibit any other clinically evident anomalies. Nevertheless, a screening audiogram revealed a mild but bilateral sensorineural hearing loss. The patient was treated with testosterone until age 39 years, when he was switched to combined gonadotropin therapy in order to induce spermatogenesis. Following IVF, he had one healthy daughter. Family history was unremarkable for pubertal timing and sense of smell in the patient's parents as well as in his two siblings. Genetic testing did not reveal any

pathogenic or likely pathogenic variants in known CHH genes. The proband is, however, a carrier of a very rare *NOS1* mutation. Both parents were deceased at the time of referral and thus could not provide a DNA sample for genetic testing.

Family F, Patient II-1

***NOS1*, p.Ile1223Met (heterozygous)**

This female patient of Portuguese origin presented at age 17 years with primary amenorrhea. Initial hormonal assessment showed low serum estradiol associated with low gonadotropins (LH < 0.1 U/l, FSH 0.23 U/l). The testing of other pituitary axes was normal. Cranial MRI showed normal pituitary gland with intact olfactory bulbs and olfactory strips. The patient has a slight intellectual deficiency. She has an apparent narrowing of the bony internal acoustic pores bilaterally with moderate hearing impairment of the left side. The sense of smell was normal based on patient's subjective assessment. A formal olfactory assessment was not performed due to subsequent hospitalization of the patient for psychiatric reasons and loss of contact with the local endocrinologist. Family history was negative for pubertal delay and decreased sense of smell. The patient does not harbor variants in known CHH genes. We detected, however, the presence of a heterozygous *NOS1* variant, inherited from her mother.

HUMAN TISSUES

Human hypothalamic tissues were obtained at autopsies from the Forensic Medicine Department of the University of Debrecen, Hungary, with the permission of the Regional Committee of Science and Research Ethics (DEOEC RKEB/IKEB: 3183-2010).

Permission to use 9 gestational-week-old human Fetuses was obtained from the French Agence de Biomédecine (PFS16-002).

Processing of human tissues and immunochemistry protocols are detailed below.

GENETIC ANALYSES

Genomic DNA was extracted from peripheral blood samples using the Puregene Blood Kit (Qiagen), following the manufacturer's protocol. Exome capture was performed using the SureSelect All Exon capture v2 or v5 (Agilent Technologies, Santa Clara, CA USA) and sequenced on the HiSeq2500 (Illumina, San Diego CA USA) at BGI (BGI, Shenzen, PRC). Raw sequences (FASTQ files) were analyzed using an in-house pipeline that utilizes the Burrows-Wheeler Alignment algorithm (BWA)(*82*) for mapping the reads to the human reference sequence (GRCh37), and the Genome Analysis Toolkit (GATK)(*83*) for the detection of single nucleotide variants (SNVs) and insertion/deletions (Indels). The resulting variants were annotated using Annovar version 20191024(*84*) and dbNSFP version 4.0(*85*) for minor allele frequency (MAF) and pathogenicity scores.

Based on the prevalence of CHH(*1*), we established the MAF threshold as 0.01% and excluded all variants with a higher MAF in gnomAD. Candidate *NOS1* variants were then prioritized using the following criteria: (1) *in silico* prediction of deleteriousness (CADD(*86, 88*) > 15), and (2) variant position in sub-regions highly intolerant to variation (LIMBR(*41*) score percentile < 5). All variants were confirmed by Sanger sequencing of both strands with duplicate PCR reactions. A gene burden analysis for the identified *NOS1* variants was performed using a two-tailed Fisher's exact test in CHH probands vs. controls (gnomAD exome controls). Furthermore, mutations in known CHH genes*(1, 42, 89)* according to ACMG criteria were noted for each proband and family members harboring rare variants in *NOS1*. More specifically, we evaluated coding exons and intronic splice regions (≤6 bp from the exons) of the known CHH genes for pathogenic and likely pathogenic variants according to ACMG guidelines (*90*). The included CHH genes are: *ANOS1* (NM_000216.2)*, SEMA3A* (NM_006080)*, FGF8* (NM_033163.3)*, FGF17* (NM_003867.2)*, SOX10* (NM_006941)*, IL17RD* (NM_017563.3)*, AXL* (NM_021913)*, FGFR1* (NM_023110.2)*, HS6ST1* (NM_004807.2)*, PCSK1* (NM_000439)*, LEP (*NM_000230), *LEPR* (NM_002303)*, FEZF1 (*NM_001024613)*, NSMF* (NM_001130969.1)*, PROKR2* (NM_144773.2)*, WDR11* (NM_018117)*, PROK2* (NM_001126128.13)*, GNRH1*

(NM_000825.3), *GNRHR* (NM_000406.2), *KISS1* (NM_002256.3), *KISS1R* (NM_032551.4), *TAC3* (NM_013251.3), *and TACR3* (NM_001059.2).

Position-specific evolutionary preservation tool (PANTHER-PSEP)(*91*) was used to determine whether the identified *NOS1* missense variants were at sites conserved among species, including *pig, rabbit, rat, mouse and ferret (GenBank accession numbers F1RKF2, O19132, D3ZEW7, Q9Z0J4 and M3XUN6 respectively*) and to predict their putative damaging effect.

IN SILICO ANALYSIS

The ConSurf web server (http://consurf.tau.ac.il) was used for the identification of evolutionary conservation of amino acid positions in human NOS1 (*92*). The degree of amino acid evolutionary conservation reflects its natural tendency to be mutated. Aim of the method was to investigate whether any of the identified mutations are important for structure and/or function based on the evolutionary pattern of Nos1. Homology sequence search was conducted based on amino acid sequence from the human crystal structure of Nos1 (PDB ID code: 5VUV). PSI-BLAST homolog search algorithm and UniProt database were used for the generation of a Multiple Sequence Alignment (MSA) with ClustalW algorithm and homologs were selected automatically. Maximum of 50 sequences, closest to the reference sequence of Nos1, were used for the analysis out of the homolog search algorithm. Maximal and minimal % ID between sequences were set at 95 and 35 respectively.

PRODUCTION OF NOS1 CONSTRUCTS

A cDNA containing the entire coding region of the human *NOS1* transcript isoform 1 (RefSeq. NM_000620.4; GenBank assembly accession; GRCh37.p13 / GCF_000001405.25), was inserted into a modified pcDNA3.1+ expression vector containing a his-tag at the 5'end (GeneCust). Similarly, plasmid encoding *NOS1* mutants (Arg260Gln and Ile1223Met) were obtained using modified pcDNA3.1+ expression vector

containing a myc-tag at the 5'end of the coding region (GeneCust). The plasmid encoding remaining *NOS1* mutants (p.Ala231Thr, p.Thr1107Met and p.Glu1124Lys) were generated by site directed mutagenesis using QuickChange XLII Kit (Stratagene) and confirmed by Sanger sequencing. FlincG3 NO-detector plasmid (pTriEx4-H6-FGAm) has been produced as described previously (*87*).

To express equimolar amounts of WT and mutated *NOS1* transcripts in transfected cells, we engineered bicistronic expression vectors encoding His-tag NOS1 and Myc-tag NOS1 separated by a P2A self-cleaving peptide to achieve equimolar expression of wild type and mutated NOS1 at single cell level (*93*). Briefly, His-NOS1 WT cassette was PCR amplified and fused via overlap PCR to a synthetic P2A DNA sequence. The resulting His-NOS1wt-P2A cassette was cloned (EcoRI – NotI) into pcDNA3.1+ expression vector. Next, sequences encoding for Myc-tag NOS1 mutants were PCR amplified adding NotI and XbaI restriction sited. PCR products were finally cloned (NotI – XbaI) to His-NOS1wt-P2A expression vectors. PCR amplifications were performed using Phusion HF (Thermo Scientific) or Herculase (Agilent Technologies) high-fidelity DNA polymerases using primers listed in Table S4. All vector sequences were validated by sanger sequencing.

COMPOUNDS USED FOR *IN VITRO* AND *IN VIVO* EXPERIMENTS

All of the compounds used were delivered to the HEK 293T cells through superfusion. To explore the ability of the transfected cell line respond to nitric oxide, cells were treated with the NO donor (Z)-1-[N-(3-ammoniopropyl)-N-(n-propyl)amino] diazen-1-ium-1,2-diolate (PAPA/NO; 1μM, Enzo Life Sciences, Exeter, UK) for a duration of 90 sec. Endogenous NO release was stimulated upon application of calcimycin (A23187; 50 nM diluted in DMSO, Abcam) for a duration of 1 min. The responses to NO could be inhibited by both the NOS inhibitor (L-NAME; 30 μM, Calbiochem) and the NO receptor blocker 1H-[1,2,4]oxadiazolo[4,3,-a] quinoxalin -1-one (ODQ; 1 μM, Sigma, Dorset, UK). ODQ is shown to selectively and potently inhibit guanylyl cyclase and thus it can block the accumulation of cGMP in response to NO donors (*94*).

For *in vivo* application NO synthesis was blocked using the NOS blocker L-NAME (Merck, Ref. 483125; 50 mg/kg i.p. and 5 mM intranasally), diluted as previously described (*95*). The activity of phosphodiesterase 5 (PDE5) was inhibited by the use of Sildenafil (SIGMA, Ref. PZ0003; 15 mg/kg, i.p.) diluted in DMSO. KINOX 450 ppm mole/mole inhaled nitric oxide gas was generously supplied by the Lille University Hospital.

CELL CULTURE OF NITRIC OXIDE DETECTOR CELLS

The HEK 293T cell line expressing NO-activated GC and phosphodiesterase-5 (PDE5), previously referred to as GChighPDE5low cells (*96*) and hereby referred to as NO detector cells, were provided by Professor Doris Koesling (Ruhr-Universitat Bochum, Bochum). HEK 293T were cultured under standard conditions in a DMEM-based medium containing 5% fetal bovine serum and appropriate selection antibiotics; they were replated before reaching 80% confluency and were passaged<35 times.

Transfection was performed on cells growing in a 12-well plate (on poly-D-lysine-coated coverslips) for live cell imaging, or in a 6-well plate for Abcam kit and co-immunoprecipitation experiments, using Fugene6 (Roche Applied Science) according to the manufacturer's protocol, in a transfection rate of 3:1 (Fugene6/DNA). For the live-cell imaging, Flincg3 plasmid was co-transfected, in a one step process, with the NOS1 plasmid used in each experiment.

WESTERN BLOT PROTEIN EXPRESSION ASSAY

HEK293 cells were transfected in 12-well plates ($2.5x10^5$ cells/well) with WT, mutant NOS1 and bicistronic constructs (500ng/well) using Fugene6 (Roche Applied Science) according to the manufacturer's protocol, in a transfection rate of 3:1 (Fugene6/DNA). After 48h, proteins were extracted and western blot performed loading 20ug per lane. NOS1 and actin were revealed using anti-myc tag HRP conjugated (1:5000; Bethyl Cat# A190-105P, RRID:AB_162712) or the anti-his tag (1:5000; Cell Signaling Technology

Cat# 2365, RRID:AB_2115720), and the anti-Actin (1/5000; Cell Signaling Technology Cat# 4970, RRID:AB_2223172) respectively.

LIVE IMAGING

***FlincG3 fluorescence imaging*:** FlincG3 has a broad excitation spectrum with peaks at 491 and 410 nM and an emission maximum at 507 nm. Time series were recorded using an Axio Observer Z1, with a camera (Orca LT) and a 20X air objective (numerical aperture 0.8, Zeiss), under software control (Zen Imaging Software, Zeiss). Fluorescent HEK 293T cells were excited at a wavelength set at 495, with an emission set at 519. Exposure levels were set at 300 ms and the intensity level at 8%. The chamber was superfused at 1.5 ml/min and temperature set at 37°C with imaging solution containing: KCl 2 mM, KH2PO4 1.18 mM, glucose 5.5 mM, HEPES 10 mM, NaCl 140 mM, CaCl2 1.5 mM. The solution was adjusted to a pH of 7.4 and osmolality to 285-290 mOsmol/kg at a temperature of 37°C.

***FlincG3 fluorescence data analyses*:** Epifluorescent signals were captured by camera, corrected for the background levels, and displayed as the change in intensity relative to baseline divided by the baseline intensity (ΔF/Fo). Peak amplitudes for each cell giving a fluorescent signal were measured by taking the maximum ΔF/Fo, subtracting the mean baseline and then subtracting the difference between the peak ΔF/Fo of the baseline and the mean baseline for that cell. These calculations were made with OriginPro software (RRID:SCR_014212).

NOS ACTIVITY ASSAY

The enzymatic activity of the NOS1 protein was assessed in NO detector cells transfected with the wild-type or the mutated plasmids, or transfected with the bicistronic constructs using a commercially available Abcam NOS activity assay kit (Cat. # ab211084) according to the manufacturer's instructions.

PROTEIN IMMUNOPRECIPITATION ASSAY

NO detector cells expressing the wild-type NOS1 or each of the bicistronic constructs stated above were lysed in Tris buffer pH 8.0 (25mM Tris base, 300mM NaCl, 50mM Imidazole) with the addition of the protease and phosphatase inhibitor cocktail (Sigma-Aldrich, Cat. # PPC1010). Histidine-tagged NOS1 was isolated using the Dynabeads His-tag isolation and pulldown kit (Invitrogen, Cat. # 10103D). Briefly 2mg of Dynabeads were added into 35μg of cell lysate and the Dynabeads-lysate mix was then incubated in a roller at 4 °C for 10min. The beads were thoroughly washed four times in the Tris buffer using a magnet and eventually any protein bound to the his-tag was eluted using Tris buffer pH 8.0 containing increased concentration of imidazole (25mM Tris base, 300mM NaCl, 500mM Imidazole). Protein content was measured in the whole lysate (i.e. prior to elution), as well as in the eluted part, using a BCA kit, according to the manufacturer's instructions. For the immunoblot of the whole lysate and the eluted proteins, loading buffer (E-Gel™, 1X, Thermo Fisher, Cat. # 10482055) was added to the 5mg of each protein sample. The mix was then boiled for 5 min before electrophoresis at 120V for 100 mins in 5–12% tris-acetate precast SDS-polyacrylamide gels according to the protocol supplied with the NuPAGE system (Thermo Fisher). After size fractionation, the proteins were transferred onto a PVDF membrane (0.2μm pore size, LC2002; Invitrogen, Carlsbad CA, USA) in the blot module of the NuPAGE system maintained at 1A for 75 min at room temperature (RT). Blots were blocked for 1h in tris-buffered saline with 0.05% Tween 20 (TBST) and 5% non-fat milk at RT, incubated for 48h at 4°C with anti-his-tag mouse monoclonal (1:1000; Thermo Fisher Scientific Cat# MA1-21315, RRID:AB_557403), rabbit anti-NOS1 (1:1000; Thermo Fisher Scientific Cat# 61-7000, RRID:AB_2313734) and rabbit anti-GAPDH (1:5000; Sigma-Aldrich Cat# G9545, RRID:AB_796208) in TBST 5% bovine serum albumin (Sigma-Aldrich, Cat# A7906), and washed four times with TBST before being exposed to horseradish peroxidase-conjugated secondary antibodies [anti-mouse Ig-HRP 1:1000 (Agilent Cat# P0260, RRID:AB_2636929) and anti-rabbit Ig-HRP 1:2000 (Agilent Cat# P0448, RRID:AB_2617138)] diluted in 5% non-fat milk TBST for 1h at RT. The immunoreactions were detected with enhanced chemiluminescence (NEL101; Perkin Elmer, Boston, MA).

ANIMALS

All C57Bl/6J mice were housed under specific pathogen-free conditions in a temperature-controlled room (21-22°C) with a 12h light/dark cycle and ad libitum access to food and water. Experiments were performed on male and female C57BL/6J mice (Charles River Laboratories), *Nos1*-deficient (*Nos1*$^{-/-}$, B6.129S4-Nos1tm1Plh/J, RRID:IMSR_JAX:002986) mice(*26*) and *Gnrh*::*Gfp* mice (a generous gift of Dr. Daniel J. Spergel, Section of Endocrinology, Department of Medicine, University of Chicago, IL)(*97*). *Nos1*$^{-/-}$; *Gnrh*::*Gfp* mice were generated in our animal facility by crossing *Nos1*$^{-/+}$ mice with *Gnrh*::*Gfp* mice. Animal studies were approved by the Institutional Ethics Committees for the Care and Use of Experimental Animals of the Universities of Lille, Bordeaux and Geneva; all experiments were performed in accordance with the guidelines for animal use specified by the European Union Council Directive of September 22, 2010 (2010/63/EU) and the Swiss Federal Act on Animal Protection Ordinance, and were approved by the French Department of Research (APAFIS#2617-2015110517317420v5 and #27300-2020092210299373v3) and the Swiss Animal Protection.

GONADECTOMY OF MICE

The gonadectomy of wild-type C57Bl/6J mice was performed either at P12 or at 13 weeks of age under general isoflurane anesthesia (induction 4% in air 2 L/min, then 1.5% in air 0.3 L/min) after local injection of lidocaine (30 microliters of a 0.5% solution, s.c.) and preemptive Meloxicam treatment (5 mg/kg). Infantile mice were killed at P23 and adults two weeks thereafter.

EXAMINATION OF PHYSIOLOGY

Weaned female mice were checked daily for vaginal opening. After vaginal opening, vaginal smears were collected daily and analyzed under the microscope to identify the puberty onset (i.e. first appearance of two consecutive days where vaginal smears contained cornified cells) and eventually the specific day of the estrous cycle. Male mice were checked daily for balanopreputial separation, as an external sign of puberty onset.

IN UTERO INTRANASAL INJECTION OF L-NAME

Pregnant wild-type females were anesthetized with isoflurane, placed ventral side up and covered with a sterile surgical cloth. Abdominal hair was removed from a small surface around the incision. Skin and connective tissue were carefully cut and a small incision in the abdominal wall allowed the exposure of the uterine horn. Each horn was carefully pulled out of the abdomen and placed on top of it, while it was kept moist with fresh DPBS throughout the surgical process. Saline and the NOS inhibitor L-NAME (5mM) were injected into contralateral horns of each pregnant female. The needle was positioned vertically over the nose of the E12.5 embryo, and introduced until it was estimated to reach the nasal septum. Following administration of the substance, the needle was held steady for a few seconds before being gently withdrawn. The uterus was then returned to the abdomen and rehydrated with a small amount of DPBS. The incisions were closed with surgical sutures and the female was singly housed until embryo harvesting (E14.5).

INTRAPERITONEAL INJECTION OF L-NAME IN INFANTILE MICE

P10 wild-type female mice received bi-daily injections of L-NAME (50 mg/kg, i.p.) or control saline, during infantile period, till the day of weaning (P21). L-NAME or the control where administered at 8H00 and 18H00, i.e. one hour after lights on and one hour before lights off according to a previously described protocol [23]. In the end of the treatment with the NOS inhibitor, mice were monitored for the assessment of pubertal onset and the study of estrous cyclicity (see “Examination of physiology” section above). When L-NAME treated mice and their control littermates reached adulthood, blood samples were collected from the facial vein on diestrus I and proestrus for the measurement of LH hormone (described below).

HORMONAL LEVEL MEASUREMENTS

Plasma LH was measured using a highly sensitive Enzyme-linked Immunosorbent Assay (ELISA) as described elsewhere (*98*). Serum FSH levels were measured using radioimmunoassay as previously described (*33*). The accuracy of hormone measurements was confirmed by the assessment of rodent serum samples of known concentration (external controls). Serum 17β-estradiol concentration was determined by ELISA (Demeditec Diagnostics, Cat# DE2693) as described previously (*99*). Inhibin B was measured using a commercial Enzyme-linked Immunosorbent Assay (ELISA) multispecies kit (AnshLabs, Cat# AL-163), following the manufacturers' protocol. AMH was measured using the commercial rat and mouse AMH Enzyme-linked Immunosorbent Assay (ELISA) kit (AnshLabs, Cat# AL-113) as described elsewhere (*100*).

INHALED NO ADMINISTRATION

Protocol was adapted from previous publications by others (*101, 102*). *Nos1*$^{+/-}$ mother with her pups (*Nos1*$^{+/+}$, *Nos1*$^{+/-}$ and *Nos1*$^{-/-}$) was placed inside a cage ("inhaled NO chamber") constantly perfused with 20 ppm NO, a dose commonly administered to premature infants at birth (*103*) that induces the production of cGMP (Figure S7). Treatment started when pups reached P10 (lights on) and ended at P23, when mice were weaned and removed from the inhaled NO chamber.

SILDENAFIL ADMINISTRATION

P10 *Nos1*$^{+/+}$, *Nos1*$^{+/-}$ and *Nos1*$^{-/-}$ mice received daily injections of the phosphodiesterase 5 inhibitor Sildenafil (15 mg/kg, i.p.) during infantile period, till the day of weaning (P23). Sildenafil was administered at 8H00, i.e. one hour after lights are on. At the end of the treatment with the NOS inhibitor, mice were monitored for the assessment of vaginal opening, pubertal onset and balanopreputial separation (see "Examination of physiology" section above).

BEHAVIORAL TESTS (COGNITION, OLFACTION, HEARING)

For all behavioral tests, the animals were coded so the investigator was blind to the genotype/phenotype of each animal.

Novel object recognition test: Recognition memory was assessed using the novel object recognition (NOR) test. During the habituation phase on day 1, each mouse was allowed to explore the open-field arena for 30 minutes. On day 2, two identical objects (A+A) were placed within the open-field arena on opposite sides of the cage, equidistant from the cage walls. Each mouse was placed within the two objects and allowed to explore them for 15 minutes. Day 3 consisted of two phases, a familiarization and a test phase. During the familiarization phase (trial 1) that lasted 15 minutes, mice explored two other identical objects (B+B). After this phase, the mouse was placed back in its home cage for 1 hour before starting the test phase. During the test phase, one object of trial 1 and a completely new object (B+C) were placed within the open-field area and mice were allowed to explore them for 5 minutes (trial 2). The object recognition score was calculated as the time spent exploring the new object (trial 2) over the total exploration time, and is used to represent recognition memory function. NOD was performed in the afternoon in 3- to 8-month-old male and female mice; females were in diestrus during the test phase.

Olfactory habituation/dishabituation test*:* The habituation/dishabituation test was used to assess the ability to differentiate between different odors. This olfactory test included a presentation of acetophenone (Sigma-Aldrich, Cat. # 00790) for habituation and octanol (Sigma-Aldrich, Cat. # 05608) for dishabituation, or vice versa. Before the test, mice were allowed to explore the open-field area and an empty odor box for 30 minutes. After this habituation period, mice were sequentially presented with one odor for four consecutive trials for a duration of 1 minute, and an inter-trial interval of 10 minutes was maintained to ensure the replacement of the odor. After four consecutive trials, a second odor was presented during a 1-minute trial. Odors (20µl of 1:1000 dilution) were administered on a filter paper and placed in a perforated plastic box, to avoid direct contact with the odor stimulus. Measures consisted in recording the total amount of time the mouse spent

sniffing the object during the different trials. Habituation/dishabituation test was performed in the morning in 3- to 8-month-old male and diestrous female mice.

***Social olfactory preference test**:* Social olfactory preference test consisted of two phases, a familiarization and a test phase. During the familiarization phase, all mice were allowed to freely explore the open-field arena and were exposed to urine samples from an adult C57BL6/J wild-type stud male and estrous female for 30 min. After 30 min in clean bedding, mice were allowed to explore the same urine samples for 10 min, during which the behavior towards the urine samples was recorded. For each test, 50 μl of either male or female urine was administered on a filter paper and placed in a perforated plastic box, to avoid direct contact with the odor stimulus. The distribution of the time sniffing the urine samples was used as an indication of the interest to gain further information from the scent source. Social olfactory preference test was performed in the morning in 3- to 8-month-old male and female mice; females were in estrous during the test phase.

Hearing tests: Mice were anesthetized by intraperitoneal injection of a mixture of ketamine and levomepromazine (100 mg/kg and 5 mg/kg respectively) and placed on a servo-controlled heating pad that maintained their core temperature at 37°C. Audiological tests were performed in a sound-proof booth. Distortion-product otoacoustic emissions (DPOAES) probes cochlear mechanics and auditory brainstem-evoked response (ABR) thresholds and suprathreshold waveforms, both of which are sensitive to detect auditory-pathway disorders. The predominant DPOAE at frequency $2f_1$-f_2 was recorded in response to two primary tones f_1 and f_2, with f_2/f_1 = 1.20, at equal sound levels (Cub^{e}Dis system, Mimosa Acoustics; ER10B microphone, Etymotic Res.). Frequency f_2 was swept at 1/10th octave steps from 4 to 20 kHz, and DPOAE level was plotted against frequency f_2 at increasing primary tone levels, from 20 to 70 dB SPL in 10 dB steps, then to 75 dB SPL. The ABRs elicited by calibrated tone bursts in the 5-40 kHz range (repetition rate 17/s) were derived by synchronously averaging electroencephalograms recorded between subcutaneous stainless-steel electrodes at the vertex and ipsilateral mastoid, with the help of a standard digital averaging system (CED1401+). One hundred 10-ms long epochs

were averaged, except within 10 dB of the ABR threshold (defined as the smallest tone-burst level giving rise to at least one repeatable wave above background noise level, 100 nV in an anesthetized mouse), for which 300 epochs were collected. Next, ABRs in response to 10-kHz tone bursts at increasing levels, stepwise from 15 to 105 dB were collected and their waves were labelled from I to IV in chronological order, for the latency of wave II to be extracted at every stimulus level. Hearing tests were performed during the whole day in 2- to 3-month-old male and diestrus female mice.

ATTENTIONAL SET-SHIFTING TASK

The attentional set shifting (ASST) apparatus and procedures were previously described in detail (*104*). In brief, testing was performed in a homemade rectangular chamber made of Plexiglas and white PVC, 40 x 30 x 40 cm. A 15 x 30 cm area of the chamber was separated in the middle by an opaque white PVC separation, on each side of which a texture and a digging bowl (made of ceramic 3 cm height x 8 cm diameter size) were placed. In all ASST trials, two odorants presented as clean odorized bedding in two bowls and two textures presented below each bowl were randomly combined and counterbalanced, and placed in two separate compartments of the testing chamber. Various spices and herbs bought in a grocery store were used as odorants and were added to the digging medium (the volume of each odorant was mostly 0.5 % of the volume of the digging medium prepared at least 24 hours before use). Various textures were used as a second sensory dimension. Each texture material was cut to obtain rectangles of similar sizes (about 18 x 14 cm) and uniform thickness. These textures were matched by color to avoid visual bias during testing.

In each trial, only one cue, either an odor or a texture, is reinforced by a food reward hidden in the bedding (TestDiet; 20 mg sucrose pellet – Chocolate 1811223). For each trial, mice were allowed a maximum of five minutes to give an answer. The mouse was requested to meet the learning criterion, which is 80 % correct choice rate over 10

consecutive trials, and at least the six last trials had to be consecutively correct choices, to pass each block within a maximum of 90 trials. The relevant dimensions were counterbalanced.

The mouse was placed on a restricted diet from at least three weeks before the ASST. Around one gram of food was provided per mouse per day to maintain the mouse above 85 % of the initial free-feeding body weight. Before starting the ASST habituation, at least five days were used to stabilize their weight. The degree of hunger could be a potential confounding factor that may affect the duration and number of trials. The body weight was thus measured every morning and evening. The quantity of daily restricted food was strictly controlled until the day the mouse terminated all blocks of the ASST.

At least 5 days before the ASST, the mouse started habituating to the empty testing chamber for 30 minutes on three consecutive days. On the fourth day, the mouse started to habituate to dig two bowls filled with bedding, and a reward (TestDiet; 20 mg sucrose pellets) was added on each side of the separating wall to train the mouse to dig for a reward.

The ASST was conducted on two consecutive days. On day one, the mouse performed the simple discrimination (SD), the compound discrimination (CD) and the reversal of CD (CDR) blocks. On day two, the mouse performed the intradimensional set-shifting (IDS) and the extradimensional set-shifting (EDS) blocks.

The odorant bedding-filled digging bowls were placed on each side of the separating wall. The bowls were placed on texture. The bowl on the side containing the relevant and correct dimension (either odorant or texture) contained a 20 mg food pellet. After the mouse was placed on the waiting chamber, the trial with the recording started. The trial ended, and its result recorded until the mouse finished having the reward sucrose pellet. If a correct choice was made, the mouse was allowed to consume the reward and then returned to the waiting chamber of the testing chamber; in case of an incorrect choice, the mouse was directly returned to the waiting chamber. If no choice was made after five minutes, the trial was considered incorrect, and the mouse had to return to the waiting chamber. For the

first three trials, the mouse was permitted to dig in the unbiased bowl without consequence, although an error was recorded, so that if one bowl was investigated in error, the mouse could move to the second baited bowl and learn the cue contingency. The location (left/right) of the digging bowls and combinations of two different textures and two different odors were pseudo-randomly changed between trials so that the mouse would not associate an odor to a texture or the correct choice to the location of the chamber. During testing, the chamber was cleaned using 70 % ethanol, and textures were cleaned after every trial. When the mouse reached a learning criterion, the next block, a new set of cues was presented, and a positive transfer of the learned rule was expected; i.e., the mouse had to make a new reward cue association within the same relevant sensory dimension as in the previous block (the SD, CD, CDR or IDS block). After reaching the learning criterion again, the next block, another set of cues was used, and a new reward-cue association was made by reinforcing a cue within the previously irrelevant dimension (the EDS block), i.e., testing the negative transfer of a previously learned rule. A perseverative response which is indicated by a continued choice using the previously learned rule, the perseverative error was computed by the total number of errors made by the mouse during first half of all trials divided by the half of the total number of trials made by the mouse to meet the criterion.

iDISCO+ AND TISSUE TRANSPARENTISATION

***Sample preparation*:** P0 pups coming from *Nos1*$^{+/-}$ mothers were anesthetized and perfused with a fixative solution made up of 4% paraformaldehyde in PBS. The heads were postfixed in the fixative overnight, then rinsed with PBS, and subsequently decalcified in an acidic solution (10% formic acid in ddH2O) before removal of the frontal and parietal bones.

***Whole-mount immunostaining and tissue-clearing*:** An adapted iDISCO+ protocol was performed: samples underwent a gradual dehydration in ethanol, followed by overnight delipidation in 66% dichloromethane (DCM) / 33% ethanol, two rinses in ethanol, and

overnight bleaching in 7% H2O2 in ethanol. Finally, samples were rehydrated gradually in ethanol and washed in KPBS. Next, the heads were blocked and permeabilized in blocking solution (KPBS + 0.2% Gelatin + 1% Triton X-100 + 0.05% NaN3) for 5 days, and incubated with primary antibodies rat anti-GnRH (1:10000 #EH1044, produced by Erik Hrabovszky) and goat anti-TAG1 (1:500, R and D Systems Cat# AF4439, RRID:AB_2044647) in blocking solution for 10 days. After several KPBS rinses, the heads were incubated with secondary antibodies in blocking solution for 5 days, and rinsed again several times in KPBS. Following immunostaining, the samples were gradually dehydrated in ethanol and left overnight in DCM 66% / 33% ethanol. The samples were finally rinsed in 100% DCM for 1 hour, before clearing in dibenzyl ether until transparency was achieved.

Light-sheet imaging and 3D-analysis: Cleared samples were imaged in dibenzyl ether on an Ultramicroscope 1 (LavisionBiotec) equiped with an Andor Neo camera and a 1.1x/0.1NA MI PLAN objective (LavisionBiotec). Acquisitions were saved as a tiff sequence, which was converted to the Imaris file format and further processed in Imaris 9.6 (Bitplane RRID:SCR_007370). The Spots tool was used for GnRH neurons counting.

IMMUNOHISTOCHEMISTRY/IMMUNOFLUORESCENCE

MOUSE

Tissue preparation: Embryos were washed thoroughly in cold 0.1 m PBS, fixed in fixative solution [4% paraformaldehyde (PFA), in 0.1 m PBS, pH 7.4] for 6–8 h at 4°C and cryoprotected in 20% sucrose overnight at 4°C. The following day, embryos were embedded in OCT embedding medium (Tissue-Tek), frozen on dry ice, and stored at −80°C until sectioning. Tissues were cryosectioned (Leica cryostat) sagitally at 16 µm.

Postnatal (P7 to P23) wild-type female mice were anesthetized with 50-100 mg/kg of Ketamine-HCl and perfused transcardially with 2-10 ml of saline, followed by 10-50 ml of 4% PFA, pH 7.4. Brains were collected, postfixed in the same fixative for 2h at 4°C, embedded in OCT embedding medium (Tissue-Tek), frozen on dry ice, and stored at

−80°C until cryosectioning (Leica cryostat). Sections were collected coronally at 35µm (free-floating sections) and 16µm for iNO box post-weaning *Nos1*$^{+/-}$ mice.

Wild-type adult intact and gonadectomized mice were injected i.p. with a mixture of pentobarbital (300 mg/kg) and lidocaine (30 mg/kg) and perfused transcardially with 2-10 ml saline followed by 200 ml of 2% PFA in PB, pH 7.4, containing 0.2% picric acid. Brains were collected, cryoprotected overnight in a sucrose solution (20% in a 0.1M veronal buffer (VB), pH 7.4), embedded in Tissue-Teck, frozen in liquid nitrogen and stored at -80°C until cutting onto a cryostat (Microm). Twelve-micrometer thick coronal sections were collected onto gelatinized slides and kept at -80°C until immunolabeling.

Immunolabeling of NOS1 and P-NOS1/ cGMP neurons in mouse developing hypothalamus: As described previously (*16, 95*), sections were washed 3 times for 15 minutes each in PB 0.1M and then incubated in blocking solution (5% NDS, 0.3% Triton X-100 in PB 0.1M) for 1 hour at room temperature. Sections were incubated for 72 hours at 4°C with rabbit anti-Ser1412 phospho-Nos1 (1:500; Thermo Fisher Scientific Cat# PA1-032, RRID:AB_325020) and sheep anti-NOS1 (1:3000; generous gift from Dr. P. C. Emson, The Babraham Institute, Cambridge, UK Cat# K205, RRID:AB_2895154) or sheep antiserum to formaldehyde-fixed cGMP (1:1000; H.W.M. Steinbusch, Maastricht University). Sections were rinsed in PB and then incubated 1h at room temperature with biotinylated donkey anti-rabbit (1:500; Jackson ImmunoResearch Laboratories Cat# 711-065-152, RRID:AB_2340593) followed by incubation 1h at room temperature with streptavidin-Alexa 568 (1:500; Thermo Fisher Cat# S-11226) and Alexa 647 donkey anti-sheep (1:500; Thermo Fisher Cat# A-21448, RRID:AB_2535865), diluted in PB 0.1M. Sections were then rinsed and counterstained with Hoechst (0.0001% in PB 0.1M; 5 min), rinsed again and coverslipped under Mowiol.

Immunolabeling of NOS1 and NK3R neurons in mouse hypothalamus*:* As described previously (*16, 95*), sections were washed in VB and incubated overnight at room temperature in a cocktail of sheep anti-NOS1 (1:5000; generous gift from Dr. P. C. Emson, The Babraham Institute, Cambridge, UK Cat# K205, RRID:AB_2895154) and rabbit anti-

NK3R [1:5000; (Dr. Philippe Ciofi, INSERM, France Cat# IS-7/7, RRID:AB_2868390) allows the selective visualization in the arcuate nucleus of kisspeptin neurons by labeling their somatodendritic domain (*21*)) in VB containing 0.25% Triton X-100 (VB-TX) and 1% normal donkey serum. After washes in VB, sections were incubated for two hours at room temperature in a cocktail of Alexa 488 donkey anti-sheep (1:1000) and TRITC donkey anti-rabbit (1:1000) (both from Jackson ImmunoResearch Laboratories) in VB-TX. Sections were then rinsed and coverslipped under a 1:3 mixture of VB and glycerol, containing 0.1% para-phenylenediamine (Sigma-Aldrich).

ADULT HUMAN BRAINS

Tissue preparation: Human hypothalamic tissues from 4 male (aged 35, 36, 61 and 83 ys) and 6 female (aged 33, 58, 60, 70, 88 and 90 ys) subjects were obtained at autopsies (*post mortem* interval<24 h) from the Forensic Medicine Department of the University of Debrecen, with the permission of the Regional Committee of Science and Research Ethics (DEOEC RKEB/IKEB: 3183-2010). The included subjects were not known to suffer from neurological or endocrine disorders prior to death. Dissection and immersion-fixation of hypothalamic tissue blocks, section preparation of serial coronal sections covering also the infundibular region were carried out as previously described (*105*).

Peroxidase immunolabeling of NOS1 and P-NOS1 neurons in adult human hypothalamus: Dissection and immersion-fixation of hypothalamic tissue blocks, section preparation and immunohistochemical procedures were adapted from previous studies (*106*). NOS1 synthesizing neurons were detected with a sheep NOS1 antiserum (1:15,000, gift from Dr. P. C. Emson, The Babraham Institute, Cambridge, UK Cat# K205, RRID:AB_2895154) and p-NOS1 neurons with a rabbit anti-Ser1412 phospho-Nos1 antiserum (1:100; Thermo Fisher Scientific Cat# PA1-032, RRID:AB_325020). A 48h incubation in these primary antibodies was followed by working dilutions of biotinylated secondary antibodies (1:500; 1 h ; Jackson ImmunoResearch Laboratories) and then, ABC Elite reagent (1:1000; 1 h ; Vector, Burlingame, CA, USA). The signal was visualized

with Nickel-diaminobenzidine (Ni-DAB). To study the relationship between NOS1 and GnRH neurons, the Ni-DAB signal was silver-gold-intensified (*106*), followed by the detection of GnRH neurons with a guinea pig GnRH antiserum (1:50,000; 48h ; #1018 produced by Erik Hrabovszky), biotin-SP–anti-guinea pig IgG (1:500; 1h ; Jackson ImmunoResearch Laboratories), ABC Elite reagent (1:1000; 1 h; Vector Laboratory) and DAB chromogen.

Triple-immunofluorescent detection of kisspeptin, NOS1 and GnRH in adult human brains: Biotin Immunofluorescence experiments were performed as reported previously (*105*). For simultaneous triple-immunofluorescent labelling of NOS1, GnRH and kisspeptin, previously characterized primary antibodies were applied to the sections in a cocktail consisting of rabbit kisspeptin (1:1000; Antibody Verify, Las Vegas, NV USA; AAS26420C) (*107*), sheep NOS1 antiserum (1:1000, gift from Dr. P. C. Emson, The Babraham Institute, Cambridge, UK Cat# K205, RRID:AB_2895154) and guinea pig GnRH (1:1000; #1018 produced by Erik Hrabovszky) (*106*) (4C; 24h). Then, the sections were transferred into a cocktail of antirabbit- Cy3 (1:1000) +anti-sheep-FITC (1:250) + anti-guinea pig-Cy5 (1:500) secondary antibodies (Jackson ImmunoResearch Laboratories) for 12 h at 4 °C. The triple-labeled specimens were mounted, coverslipped with Mowiol and analyzed with confocal microscopy (Zeiss LSM780 microscope). High resolution images were captured using a 20×/0.8 NA objective, a 1–3× optical zoom and the Zen software (Carl Zeiss). Different fluorochromes were used and detected with the following laser lines: 488 nm for FITC, 561 nm for Cy3, 633 nm for Cy5.

Emission filters were as follows: 493–556 nm for FITC, 570–624 nm for Cy3 and 638–759 nm for Cy5. To avoid the emission crosstalk between the fluorophores, the red channel (Cy3) was recorded separately from the green (FITC)/far-red (Cy5) channels ('smart setup' function). To illustrate the results, confocal Z-stacks (Z-steps: 0.941-1.000 µm, pixel dwell time: 1.27-1.58 µs, resolution: 1024×1024 pixels, pinhole size: set at 1 Airy unit) were used. The extent of colocalization between kisspeptin and NOS1 was estimated from four

subjects (aged 58, 70, 88 and 90 ys) of the postmenopausal model known to exhibit the highest kisspeptin levels in the infundibular region (*106*).

DIGITAL IMAGE ACQUISITION OF MOUSE SECTIONS

Immunofluorescent preparations were analyzed on the LSM 710 Zeiss confocal microscope. Excitation wavelengths of 493/562 nm, 568/643 and 640/740 were selected to image Alexa 488, Alexa 568 and Alexa 647 secondary antibodies. All images were taken with the objective EC Plan-Neofluar M27 (thread type). For investigating GnRH neuronal migration in embryonic tissue, sagittal sections of the head were acquired with the 20X objective, using a numerical aperture 0.50, and a zoom of 1.0. For the analysis of hypothalamic NOS1/p-NOS1 ratio during development, Z-stack images were acquired with the 40X oil objective, using a numerical aperture of 0.50, and a zoom of 1.0. For the analysis of hippocampal NOS1/p-NOS1 ratio after ovariectomy, Z-stack images with tiles were acquired with the 20X objective, using a numerical aperture of 0.80, and a zoom of 1.0 All images were captured in a stepwise fashion over a defined z-focus range corresponding to all visible staining within the section and consistent with the optimum step size for the corresponding objective and the wavelength. Two-dimensional images presented here are maximal intensity projections of three-dimensional volumes along the optical axis. Illustrations were prepared using Adobe Photoshop (Adobe Systems, San Jose, CA).

CELL COUNTING

Analysis was undertaken by counting the numbers of single-labeled, dual-labeled (NOS1 staining colocalizing with p-NOS1). The number of the above Nos1- expressing neuronal populations were counted in the region of organum vasculosum lamina terminalis (OVLT), represented by plate 16, of the L.W. Swanson brain map(*108*) as described previously(*15*). All the above values for each mouse were used to determine mean counts for each age group which were then used to generate mean + SEM values for each group. Embryonic

tissue sagittal sections of the brain were examined in a Zeiss Axio Imager Z2 microscope. Alexa 488 was imaged by using a 495 beam splitter with an excitation wavelength set at 450/490 and an emission wavelength set a 500/550, allowing the identification of immunocytochemically labeled GnRH neurons. All GnRH neuronal nuclei throughout each tissue section were visualized and counted.

ISOLATION OF HYPOTHALAMIC GnRH NEURONS USING FLUORESCENT-ACTIVATED CELL SORTING

To obtain single-cell suspensions the preoptic region of *Nos1*$^{-/-}$; *Gnrh*::*Gfp*; mice was microdissected and enzymatically dissociated using a Papain Dissociation System (Worthington, Lakewood, NJ). FACS was performed using an EPICS ALTRA Cell Sorter Cytometer device (BD Bioscience). The sort decision was based on measurements of GFP fluorescence (excitation: 488nm, 50 mW; detection: GFP bandpass 530/30 nm, autofluorescence bandpass 695/40nm) by comparing cell suspensions from *Gnrh*::*Gfp* and wild-type animals. For each animal, approximately 200 GFP-positive cells were sorted directly into 10µl extraction buffer: 0.1% Triton® X-100 (Sigma-Aldrich) and 0.4 U/µl RNaseOUT™ (Life Technologies).

QUANTITATIVE RT-PCR ANALYSES

mRNAs obtained from FACS-sorted GnRH neurons or pituitary tissues were reverse transcribed using SuperScript® III Reverse Transcriptase (Life Technologies) and a linear preamplification step was performed using the TaqMan® PreAmp Master Mix Kit protocol (P/N 4366128, Applied Biosystems). Real-time PCR was carried out on Applied Biosystems 7900HT Fast Real-Time PCR System using exon-boundary-specific TaqMan® Gene Expression Assays (Applied Biosystems): *Gnrh1* (Gnrh1-Mm01315605_m1), *Gnrhr* (Mm00439143_m1), *Cebpb* (Mm00843434_s1). Control housekeeping genes: *r18S* (18S-Hs99999901_s1), *ACTB* (Actb-Mm00607939_s1).

BRAIN SLICE PREPARATION AND ELECTROPHYSIOLOGY

Infantile *Nos1*$^{+/+}$;*Gnrh::Gfp* and *Nos1*$^{-/-}$; *Gnrh*::*Gfp* littermates (P13-P20) were anaesthetized with isoflurane, and, after decapitation, the brain was rapidly removed and put in ice-cold oxygenated (O_2 95% / CO_2 5%) artificial cerebrospinal fluid (ACSF) containing the following (in mM): 120 NaCl, 3.2 KCl, 1 NaH_2PO_4, 26 $NaHCO_3$, 1 $MgCl_2$, 2 $CaCl_2$, 10 glucose, pH 7.4 (with O_2 95% / CO_2 5%). After removal of the cerebellum, the brain was glued and coronal slices (150 µm thickness) were cut throughout the septum and preoptic area using a vibratome (VT1200S; Leica). Before recording, slices were incubated at 34ºC to recover for 1 h. After recovery, slices were placed in a submerged recording chamber (32.8ºC; Warner Instruments) and continuously perfused (2 ml/min) with oxygenated ACSF. *GFP*-positive GnRH neurons in the hypothalamic preoptic area were visually identified with a 40 X objective magnification in an upright Leica DM LFSA microscope under a FITC filter and their cell body observed by using IR-differential interference contrast. Whole-cell patch-clamp recordings were performed in current-clamp with bridge mode by using a Multiclamp 700B amplifier (Molecular Devices). Data were filtered at 1 kHz and sampled at 5 kHz with Digidata 1440A interface and pClamp 10 software (Molecular Devices). Pipettes (from borosilicate capillaries; World Precision Instruments) had resistance of 6-8 MΩ when filled with an internal solution containing the following (in mM): 140 K-gluconate, 10 KCl, 1 EGTA, 2 Mg-ATP and 10 HEPES, pH 7.3 with KOH. Bridge balance was adjusted to compensate for pipette resistance. All recordings were analyzed with Clampfit 10 (Molecular Devices). Junction potentials were determined to allow correction of membrane potential values. Electrical membrane properties were measured in current-clamp mode by applying a series of current pulses from – 60 to + 80 pA (1 s, 10 pA increments). Input resistance (R_{in}) was determined by measuring the slope of the linear portion of the current-voltage (I-V) curve. All data are presented as mean ± standard deviation.

STATISTICAL ANALYSIS

All analyses were performed using Graphpad Prism Software (San Diego, CA, RRID:SCR_002798) and assessed for normality (D'Agostino&Pearson or Shapiro–Wilk test) and variance, when appropriate. Sample sizes were chosen according to standard practice in the field. The investigators were blinded to the group allocation during the experiments. For animal studies, data following the normal distribution were compared using an unpaired two-tailed Student's *t*-test or a one-way ANOVA for multiple comparisons against the control condition followed by Dunnett multiple comparison *post-hoc* test. Data not following normal distribution were analyzed using either a Mann-Whitney *U* test (comparison between two experimental groups) or Kruskal-Wallis test (comparison between three or more experimental groups) followed by a Dunn's *post hoc* analysis. The number of biologically independent experiments, sample size, *P* values, age and sex of the animals are all indicated in the main text or figure legends as well as in the statistical excel file (see data file S1) provided. All experimental data are indicated as mean ± s.e.m. The significance level was set at $P < 0.05$ with 95% confidence interval. Symbols in figures correspond to the following significance levels: ns. $P > 0.05$, * $P < 0.05$, ** $P < 0.001$, ***$P < 0.0001$. Exact P values and further statistical analysis provided in the Table S2 and raw data in Table S3.

Supplementary Tables

NOS1 mutations	MAF in gnomAD exome datasets			Allelic count			Regional constraint	Protein prediction		
HGSV	gnomAD	gnomAD (controls)	gnomAD (controls) MaxPop	CHH M / W	gnomAD M / W	Fisher test (p value)	LIMBR (percentile)	CADD	PP2	SIFT2
c.691G>A [p.Ala231Thr]	absent	absent	absent	1 / 681	0 / 108486	0.0062	4.35%	15.01	B	T
c.779G>A [p.Arg260Gln]	0.003%	0.002%	0.006% (Latino)	1 / 681	2 / 108058	0.0187	4.35%	23.6	B	T
c.3320C>T [p.Thr1107Met]	0.007%	0.006%	0.012% (Eu non Finn)	1 / 681	7 / 108615	0.0488	1.28%	29.9	D	D
c.3370G>A [p.Glu1124Lys]	0.005%	0.006%	0.014% (Eu non Finn)	2 / 680	6 / 108250	0.0011	1.28%	22.3	B	T
c.3669A>G [p.Ile1223Met]	absent	absent	absent	1 / 681	0 / 108627	0.0062	1.28%	24	P	T

Nucleotide and protein changes are based on reference cDNA sequence NM_000620.4. CHH cohort included 341 patients. MAF, minor allele frequency. M/W, number of mutated/ wild type alleles.

Table S1: Genetic and functional characterization of *NOS1* rare sequence variants in CHH patients

Primer name	Sequence (5' – 3')
His-NOS1-F	GTCCAGTGTGGTGGAATTCGCC
His-NOS1-P2A-R	TCTCCTGCTTGCTTTAACAGAGAGAAGTTCGTGGCGGAGCTGAAAACCTCATCGG
myc-NOS1-F1	CGCTTCACGCGGCCGCTATGGAGCAGAAACTCATCTCTGAAG
myc-NOS1-F2	CGCTTCACGCGGCCGCTATGGAGCAAAAACTTATTTCAGAGG
myc-NOS1-R1	GACACCGATGAGGTTTTCAGCTCCTCTAGACGATTCAGG

Table S4: Primers used for the production of his-NOS1-P2A-myc-NOS1 expression vectors

Supplementary Figures

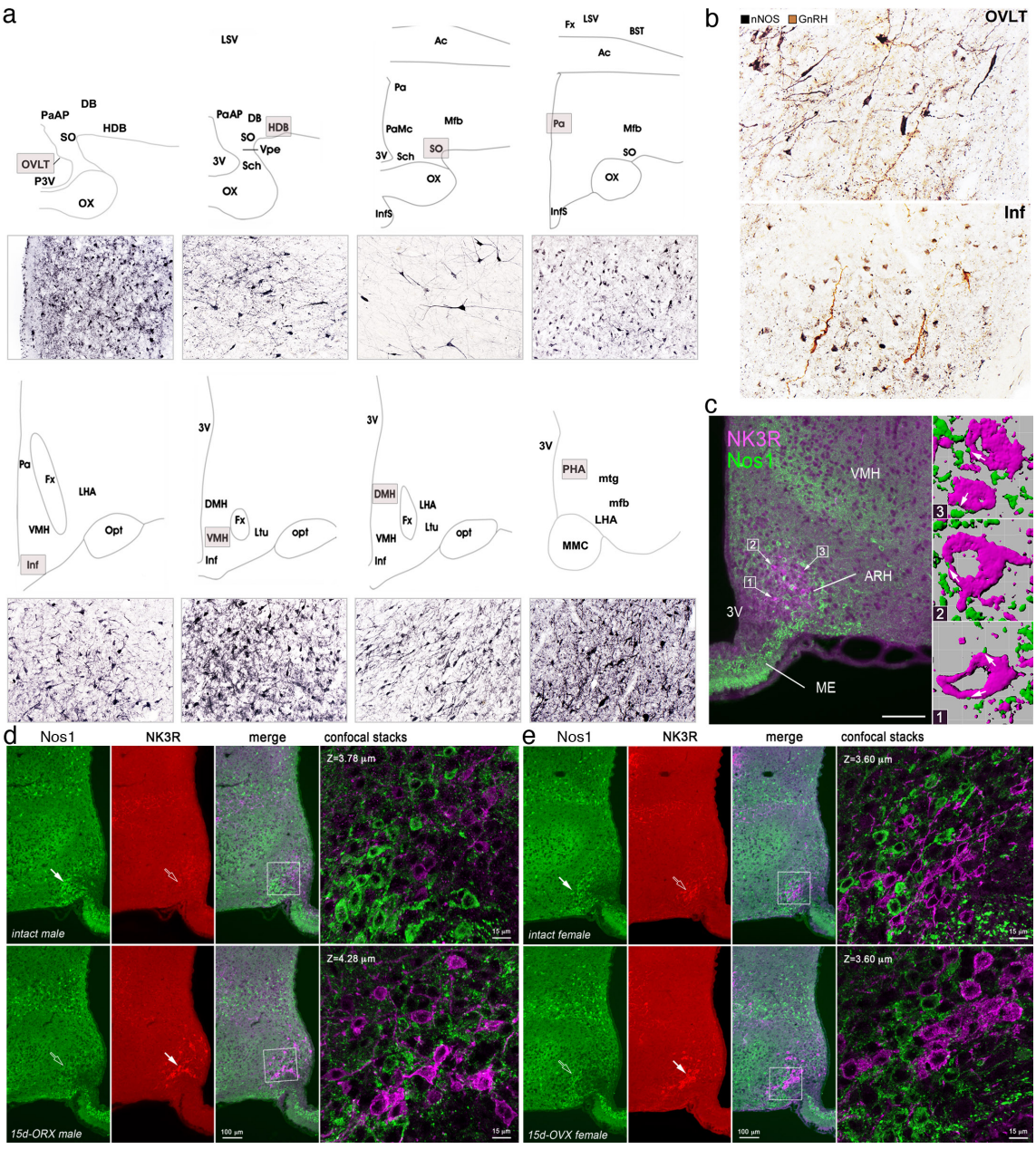

Figure S1. **NOS1 expression in the GnRH neuronal system in humans and mice**

(a) Distribution of NOS1-immunoreactive neurons (purple labeling) throughout the adult hypothalamus in human.

(b) Anatomical relationship between NOS1 neurons (purple) and GnRH neurons (light brown) in the region of the organum vasculosum laminae terminalis (OVLT, upper panel) and the infundibulum (Inf, lower panel) in adult human hypothalamus.

(c) Localization of Nos1 immunoreactivity with respect to the NK3R-immunoreactive kisspeptin neurons in the arcuate nucleus (ARH) of the hypothalamus in mice. Separate neurons display labeling for Nos1 (green) and NK3R (magenta), but their interaction is

visible under the form of putative Nos1-contacts onto NK3R-somatodendritic domains (arrows in insets numbered 1-3). *Left*, video camera image of a 12 μm-thick section. *Right*, surface renderings of confocal optical sections, 1μm-thick over a 10μm-grid. (d,e) Nos1 and NK3R immunoreactivities in intact and 2-week gonadectomized adult males (d) and females (e).

Ac, anterior commissure; BST, bed of the stria terminalis; DB, diagonal band of Broca; DMH, dorsomedial hypothalamic nucleus; fx, fornix; HDB, horizontal limb of the diagonal band; LHA, lateral hypothalamic area; LSV, lateral septal nucleus mfb, medial forebrain bundle; LTu, lateral tuberal nucleus; MMC, medial mammillary nucleus; mtg, mammillo-tegmental tract; opt, optic tract; ox, optic chiasma; Pa, paraventricular nucleus; PaAP, paraventricular nucleus anterior parvicellular; PaMC, paraventricular nucleus magnocellular part; PHA, posterior hypothalamic area; Sch, suprachiasmatic nucleus; SO, supraoptic nucleus; VMH, ventromedial hypothalamic nucleus; 3V, third ventricle. Bar, 100 μm in (a) and (c), and 50 μm in (b).

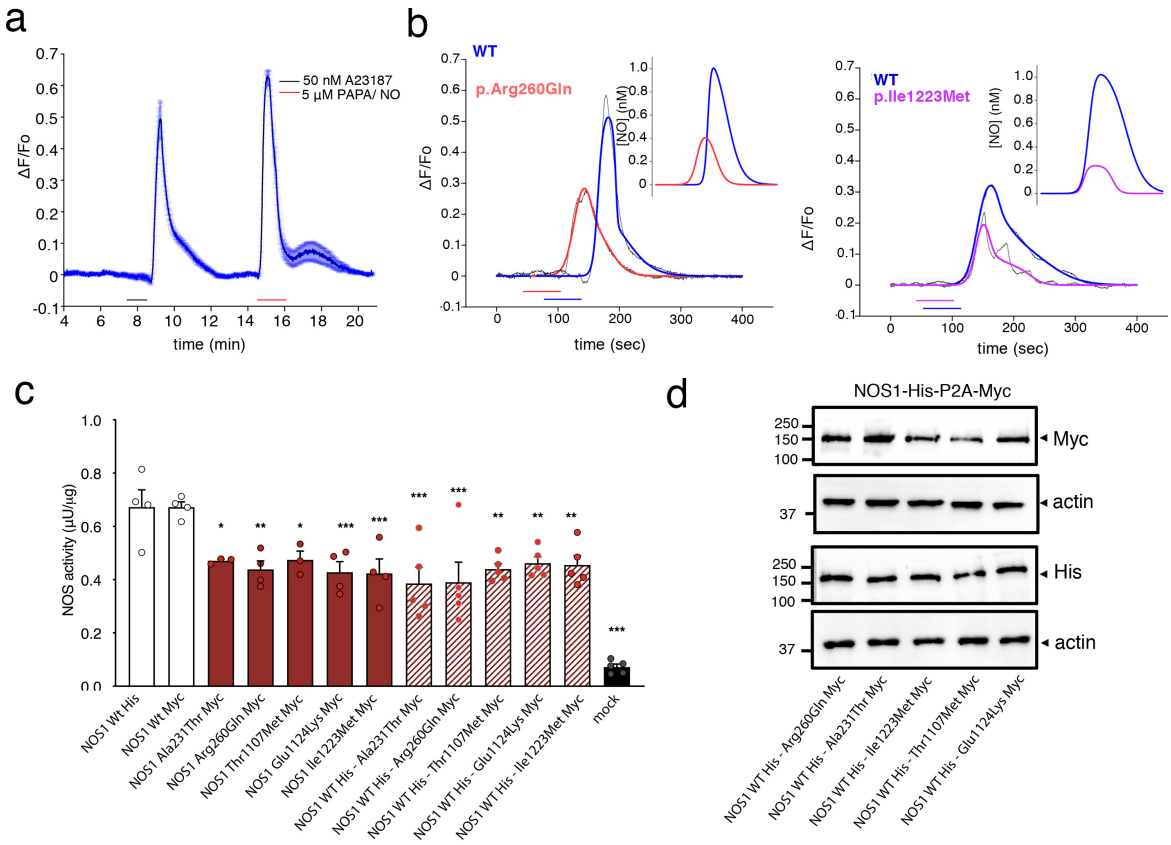

Figure S2. Functional assays of the NOS1 mutants *in vitro*.

(a) Demonstration of the experimental protocol routinely used for testing the different NOS1 variants: Superfusion of the calcium ionophore A23187 (50 nM) elicited a seemingly rapid fluorescence response that reached a peak within the first minute of the application in cells expressing the wild-type plasmid before recovering to baseline values on washout. Superfusion of a high concentration of the NO donor PAPA/NO (5 µM) allowed us to estimate the peak of the A23187-evoked increase in fluorescence using the published concentration-response curve parameters in FlincG3-transfected HEKGC/PDE5 cells. Data are means of different cells recorded from the same coverslip (n>20 for each experiment).

(b) Representative illustrations of the behavior of FlincG3-transfected HEKGC/PDE5 cells co-transfected with the wild-type or mutated NOS1 in response to application of the A23187. Mutants are illustrated in comparison to wild-type cells from the same experiment (transfection and imaging). The color-coded line (wild-type NOS1 is represented in blue and mutants are each in a different color) fits the data to the GC/PDE5 model previously published. The inset illustrates the attempts to describe NO generation using the Mathcad model, which are in good agreement with those calculated using the Hill equation (data not shown). The similarities in the shapes of the derived NO concentration profiles indicate

that the time-courses for the mutants are similar to wild-type, suggesting reduced net NO synthesis as opposed to altered activation kinetics. Note that NO release was not observed in cells not containing any NOS1 construct, while it was abolished in the presence of the guanylate cyclase inhibitor ODQ (1 μM) (data not shown).

(c) Measurement of the enzymatic activity (μU/μg) of the NOS1 protein detected in HEK GC/PDE5 cells expressing the wild-type, or the mutated (identified variants or the bicistronic plasmids) NOS1 protein, or in cells not transfected (i.e. mock cells) using a commercially available kit. Mutants are compared to wild-type values (one-way ANOVA with Dunnett's post-hoc test, n=4,4,3,4,3,4,4,5,5,5,5,5,5). * $P < 0.05$; ** $P < 0.01$; *** $P < 0.001$. Values indicate means ± SEM. N >3 independent experiments using technical replicates; each dot represents an independent experiment including technical triplicates.

(d) Representative Western blots showing Myc-tagged NOS1 mutants with His-tagged WT NOS1 in cells transfected with the bicistronic NOS1-His-PA-NOS1-Myc plasmid. Actin immunoblot was used as loading control.

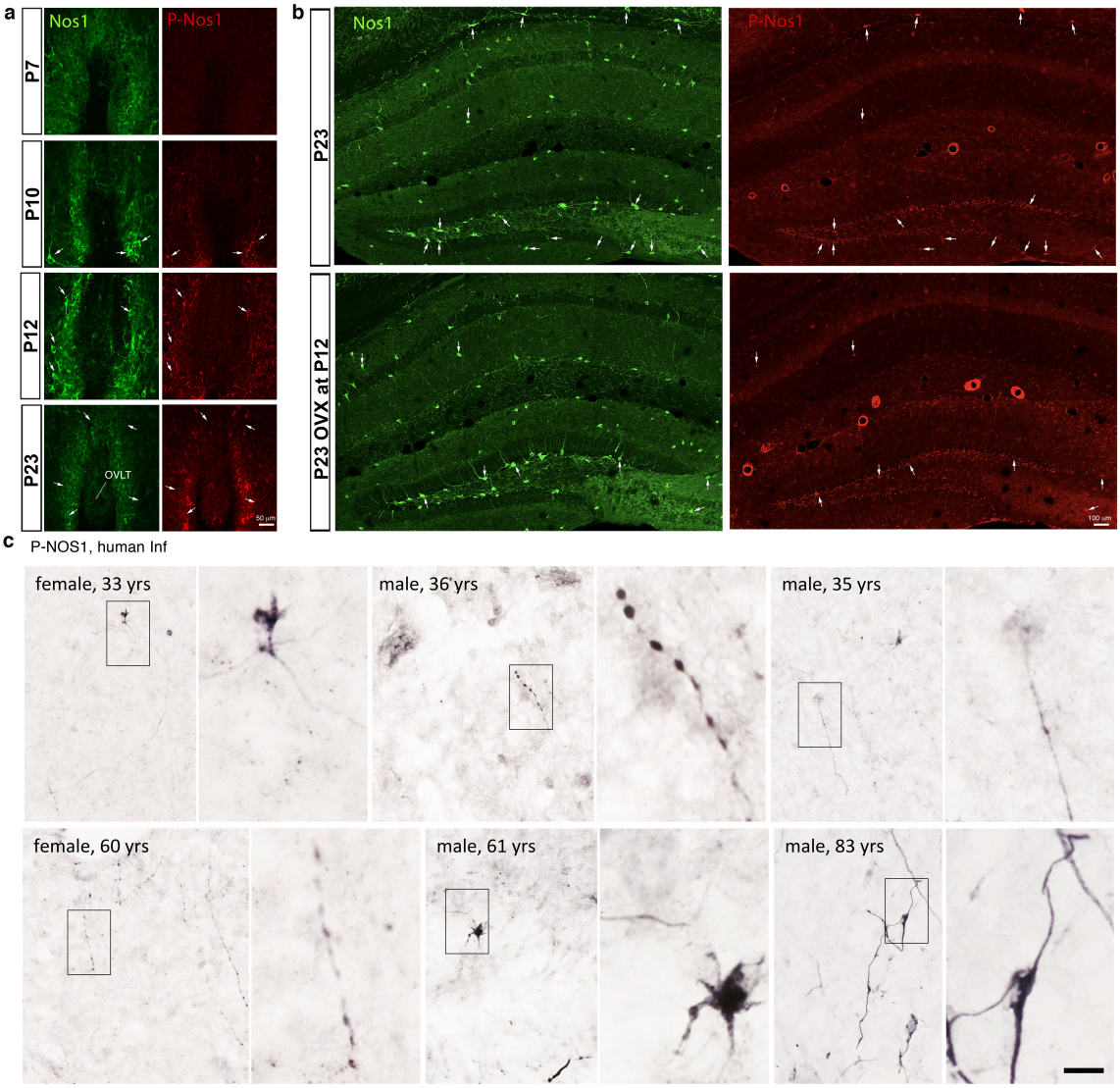

2010 **Figure S3. Immunofluorescent images of the Nos1 / P-Nos1 labeling in various areas of the mouse and human brain.**

2012 (a) Progressive phosphorylation of the Nos1 protein during postnatal development in the preoptic region at the level of the organum vasculosum of the lamina terminalis (OVLT) 2014 leads to activation of the NO pathway at postnatal day 12. Nos1 (green) and P-Nos1 (red) immunoreactivity in forebrain coronal sections of the OVLT in female mice during pre- 2016 pubertal postnatal day 7, 10, 12, and 23.

(b) Ovariectomy at p12 blunted the increase in the phosphorylation of Nos1 at P23 in 2018 the hippocampus.

(c) Representative images showing NOS1 Ser1412 phosphorylation immunolabeling in 2020 the adult hypothalamus of women and men at different ages.

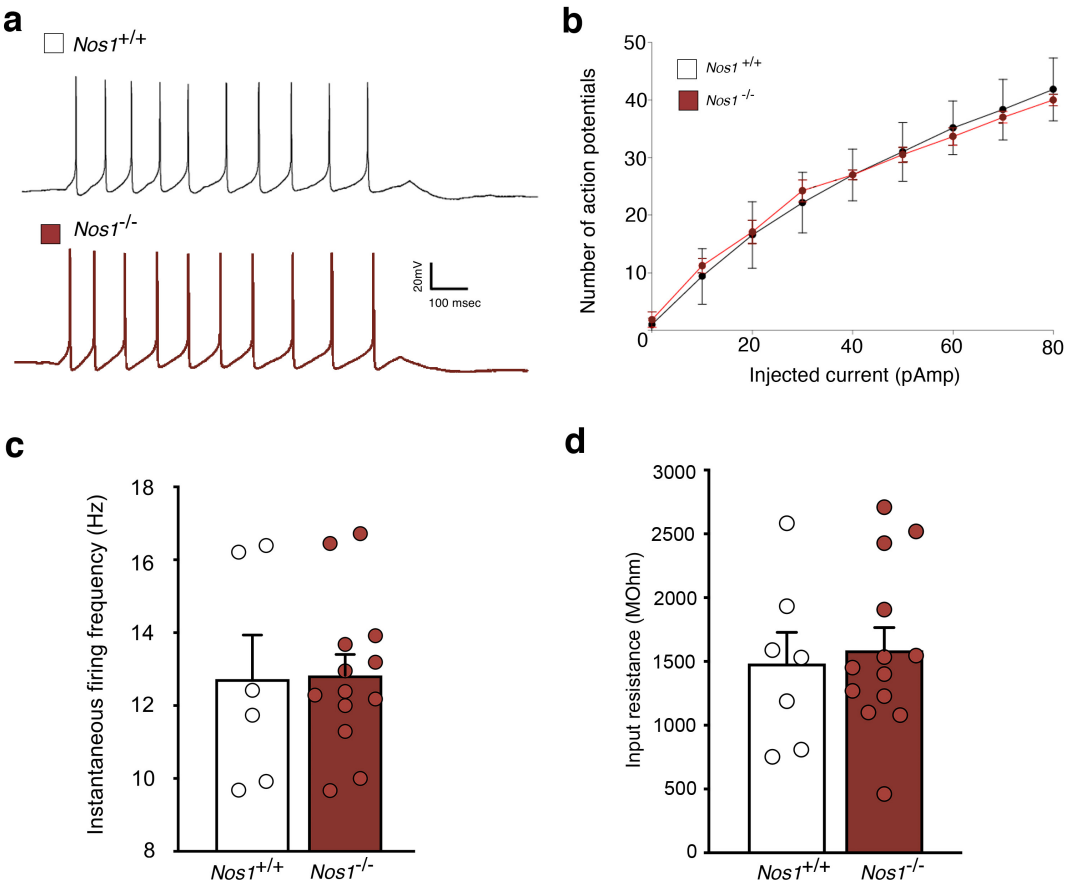

Figure S4. The increased GnRH excitability in *Nos1*$^{-/-}$ mice (Figure 5c, 5d) is not due to cell autonomous changes since the evoked firing response of GnRH neurons does not differ between *Nos1*$^{+/+}$ and *Nos1*$^{-/-}$ animals.

(a) Representative traces of firing evoked by a 10pA current injection in GnRH neurons from *Nos1*$^{+/+}$ (top trace in black) and *Nos1*$^{-/-}$ (bottom trace in brown) mice.

(b) Frequency-Current curve of evoked firing response in GnRH neurons from *Nos1*$^{+/+}$ (white) and *Nos1*$^{-/-}$ (brown) mice over a range of current injections.

(c) Instantaneous firing frequency (1/1st interspike interval) after 10pA current injection in GnRH neurons (n=6,13) from *Nos1*$^{+/+}$ and *Nos1*$^{-/-}$ animals (N=5,6).

(d) Input resistance in GnRH neurons (n=7,13) from *Nos1*$^{+/+}$ and *Nos1*$^{-/-}$ animals (N=5,6). Values indicate means ± SEM. Animals were from at least 3 independent litters.

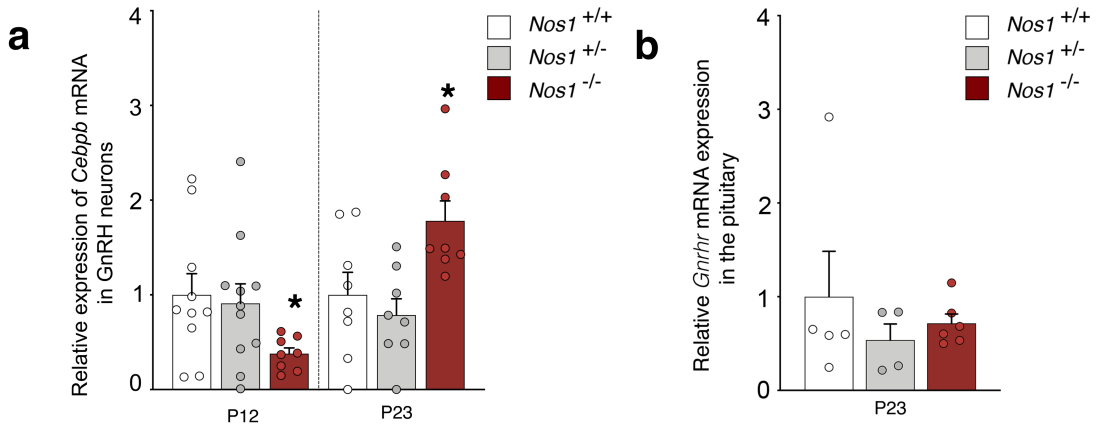

Figure S5. NOS1-deficiency alters the infantile expression of the *Gnrh* promoter repressor *Cebpb* in GnRH neurons isolated by FACS, but not *GnrhR* expression in the pituitary.

(a) *Cebpb* transcript expression in GnRH neurons at P12 and P23 in wild-type and NOS1-deficient mice. *Gnrh::Gfp; Nos1*$^{+/+}$ values are compared to those of *Gnrh::Gfp; Nos1*$^{+/-}$ and *Gnrh::Gfp; Nos1*$^{-/-}$ mice (one-way ANOVA with Dunnett's post-hoc test; P12: n=10,11,8; P23: n=8,8,8) * P<0.05. Values indicate means ± SEM. N=5-8 independent litters.

(b) *Gnrhr* transcript expression in the pituitary at P23 in wild-type and NOS1-deficient mice (n=5,4,6). Values indicate means ± SEM. N>3 independent litters.

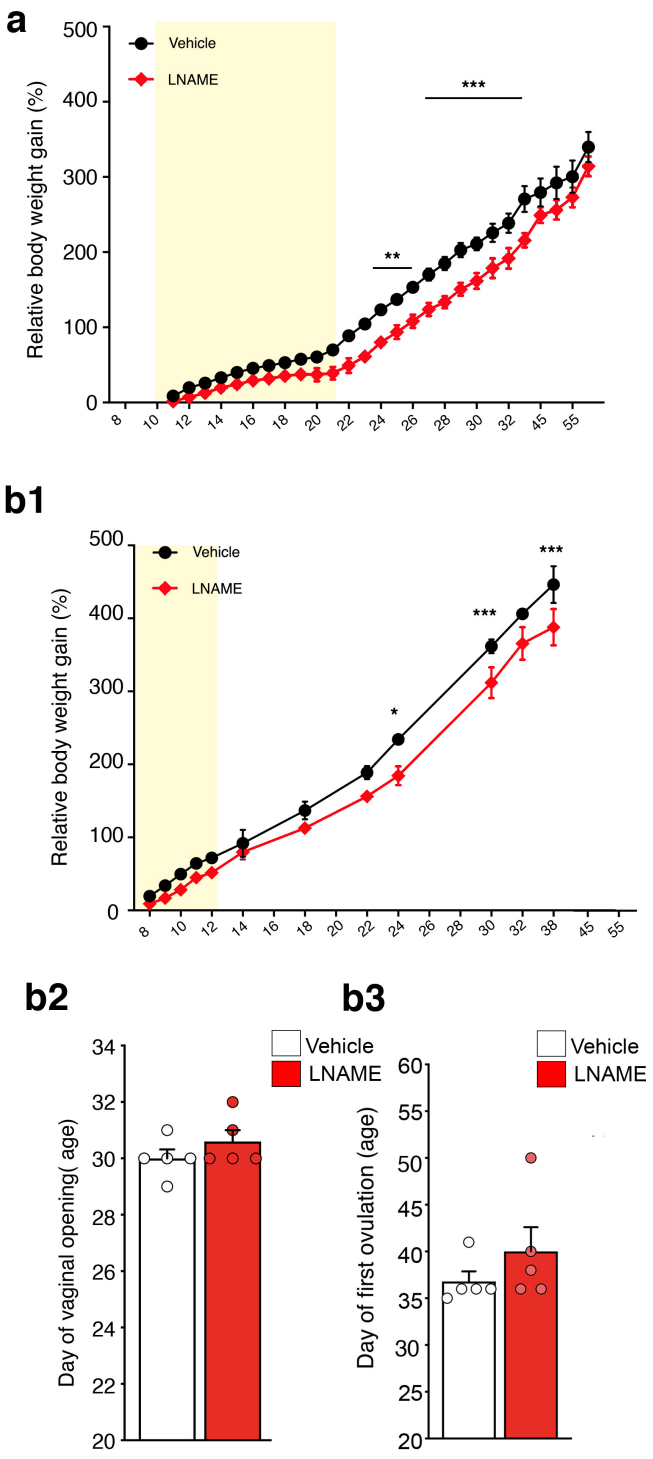

Figure S6. Pharmacological inhibition of NO synthesis during the beginning of the infantile period (P7- 12) leads to a significant decrease in body weight, whilst it has no effect on the sexual maturation. Examination of relative body weight gain (a,b1) of mice treated daily with vehicle or L-NAME between P10 and P23 (a, n=10,9) or P7 and P12 (b1, n=5,6). In the latter group of mice vaginal opening (b2) and pubertal onset in female mice (b3) were also analyzed (n=5,5). Vehicle treated animals are compared with L-NAME injected littermates using multiple t test with Holm-Sidak correction(a) or unpaired

t-test (b,c). * P < 0.05; ** P < 0.01; *** P<0.001. Values indicate means ± SEM. N>3 independent litters.

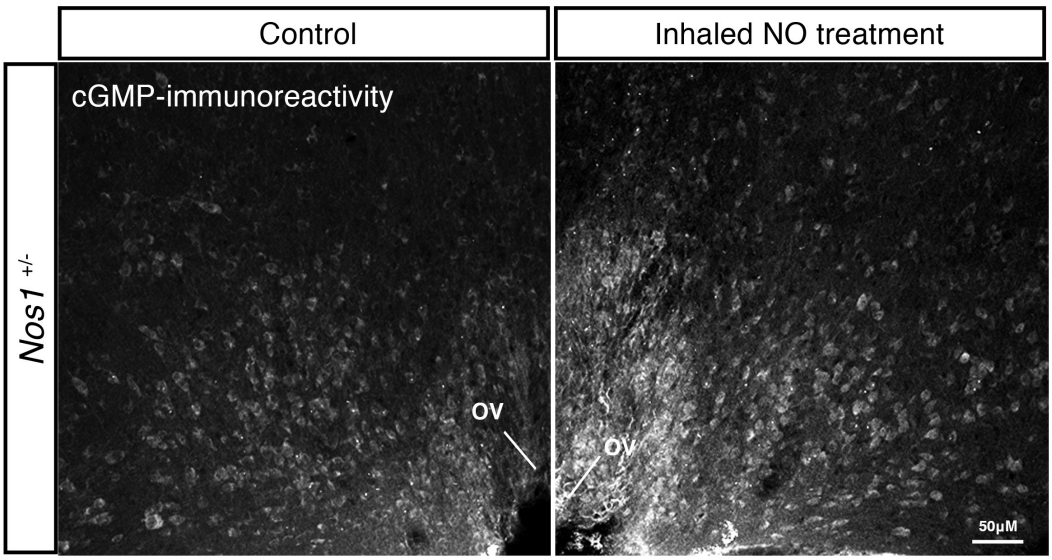

Figure S7. Representative immunofluorescent image showing increased cGMP content in the OVLT of P23 *Nos1*$^{+/-}$ male mouse after 11-d NO treatment. Immunostaining against cGMP (white) in coronal sections (16µm) from the OVLT region of a control (left panel) and inhaled NO treated (right panel) *Nos1*$^{+/-}$ male mouse. Pups treated with inhaled NO have been exposed with the whole litter to 20 ppm NO from P10 to P23. Scale bar: 50 µm.